SRTTU

Journal of Electrical and Computer Engineering Innovations

JECEI, Vol. 5, No. 2, 2017

Regular Paper

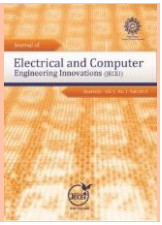

Design of a Single-Layer Circuit Analog Absorber Using Double-Circular-Loop Array via the Equivalent Circuit Model

Mojtaba Basravi[1], Zaker Hossein Firouzeh[1,*], and Mohsen Maddahali[1]

[1]Department of Electrical and Computer Engineering Isfahan University of Technology, Isfahan, Iran.
*Corresponding Author's Information: zhfirouzeh@cc.iut.ac.ir

ARTICLE INFO

ARTICLE HISTORY:
Received 19 January 2018
Revised 18 March 2018
Accepted 03 April 2018

KEYWORDS:
Frequency selective surfaces (FSS)
Circuit analogue (CA) absorber
Equivalent circuit model (ECM)
Double-circular –loop (DCL)
Angular stability.

ABSTRACT

A broadband Circuit Analogue (CA) absorber using double-circular-loop array is investigated in this paper. A simple equivalent circuit model is presented to accurately analyze this CA absorber. The circuit simulation of the proposed model agrees well with full-wave simulations. Optimization based on the equivalent circuit model, is applied to design a single-layer circuit analogue absorber using double-circular-loop array. Simple guidelines for designing the CA absorber are then formulated. It is demonstrated that the fractional bandwidth of 125.7% is realized for at least 10 dB reflectivity reduction with angular stability to 40˚ for both TM and TE modes. The total thickness of the absorber design is $0.093\lambda_L$ at the lowest operating frequency.

1. INTRODUCTION

Electromagnetic absorbers have an essential role in military and civil electronic systems. They are traditionally used to reduce the radar signature in stealth technology. In such applications, it is desired to have broadband performance, low-profile structures as well as polarization and angular insensitive response. The earliest form of radar absorber is Salisbury screen. Since it is a narrow-band device the bandwidth can be improved by Jaumann absorber, but the thickness of the absorber increases. Extremely-thin absorbers can be fabricated using materials with magnetic losses. Although the magnetic materials are typically thinner than ordinary dielectric absorbers, they are bulky and heavy because of their high concentrations of iron [1].

Recently, the frequency selective surfaces (FSS) have been widely used as circuit analogue (CA) absorber in radar absorbing materials (RAMs) for stealth technology [2]. The FSS absorbers with reactive components can provide better absorption and wider bandwidth compared with traditional absorbers [1]. The smallest thickness-to-bandwidth ratio for an absorber was formulated by Rozanov [3]. The capacitive circuit method proposed for designing wide-band absorbers are usually realized through multilayered structures.

For a single-layer absorber, a bandwidth of about 98.5% was realized with a thickness of $0.112\lambda_L$ at the lowest operating frequency [4]. In another work, a bandwidth of 112% with a thickness of $0.104\lambda_L$ was realized by using a resistive square loop as the unit cell of absorber [5]. The optimization method based genetic algorithm was used to design an absorber with embedded periodic resistive patches and achieved a bandwidth of 77.5% with a thickness of $0.091\lambda_L$ [6]. A two-dimensional periodic array with unit cells consisting of double-square loop (DSL) loaded with series resistances was also proposed by Shang et al. [7] with a bandwidth of 126.8% and a thickness of $0.088\lambda L$. However, the absorption begins to deteriorate when the incident angle is more than 30 degrees. Also, the equivalent circuit models of square-shaped FSS absorbers have been reported in [8] and [9]. In this paper, a new CA absorber which is low profile and broadband is designed to have a higher angular

stability.

To analyze the electromagnetic performance of the frequency selective surfaces, full wave methods are commonly employed [10], [11]. However, these techniques are time-consuming. Also, the designer cannot obtain any deep insight into the physics behind the structures. During the last years, many researchers have tried to derive equivalent circuit model to suitably represent these structures. For simple shapes, analytical formulas have been presented. Some models have been previously introduced for the single square [12], Jerusalem cross [13], [14] and double square loops [15].

In this paper, a novel equivalent circuit model of the CA absorber structure based on double-circular loop (DCL) frequency selective surfaces is presented. The DCL structure with a grounded substrate is a CA absorber whose frequency response is insensitive to high incident angle variations. The model can be expressed as two resonators connected in parallel with short-circuited transmission line. In addition, the bandwidth of the absorber structure is analyzed and optimization is performed based on the equivalent circuit model (ECM). The proposed model is used to design a broadband single-layer circuit CA absorber with the DCL array. For this purpose, an objective function is defined based on the reflection coefficients throughout the desired bandwidth. The optimized structure is simulated, and compared to analytical results.

The paper is organized as follows. Section 2 introduces the structure of the double-circular-loop absorber and the equivalent circuit model. The design guidelines are presented in Section 3. Physical interpretation of the absorber design is given in section 4. Section 5 illustrates the performance of the proposed FSS absorber. Finally, the concluded remarks are given in Section 6.

2. Absorber Structure and Equivalent Circuit Model

In order to design a thin and broadband EM absorber, lossy frequency selective surfaces are employed to achieve high absorption and angle stability for different polarizations over the whole frequency range of interest. The geometry of the proposed FSS absorber is depicted in Fig. 1. In each unit cell, there are two printed circular conducting loops loaded with lumped resistors. The thickness of the spacer between the ground and the lossy layer is h_1 with the relative permittivity of about 1. Therefore, it can be regarded as air or foam.

Copper is used as a lossy metal to realize circular loops because copper is inexpensive and available compared to other lossy metals. Note that a very thin layer of FR4 with thickness of h_2 is used to print the loops on its top plane. Eight lumped resistors are inserted in the inner (Res_{in}) and outer (Res_{out}) circular loops with the radius of R_{in} and R_{out}, respectively. For FR4 layer, ε_{r2}=4.3 and h_2=0.25mm and the foam with ε_{r1}=1.03 is used as the spacer.

Full wave analysis methods for FSS problems might yield a time-consuming computation in which optimization algorithms cannot be used easily. In this study, a simple equivalent circuit model is derived and proposed for the absorber structure instead of analysing the absorber performance with complicated full-wave software. The model is valuable to predict the frequency response and carry out parametric studies.

A. Equivalent circuit model for double-circular-loop FSS

The ECM is proposed according to the theory proposed by Marcuvitz [16], who developed the initial expressions for the periodic gratings. This technique was first used by Anderson [17] for frequency selective surfaces.

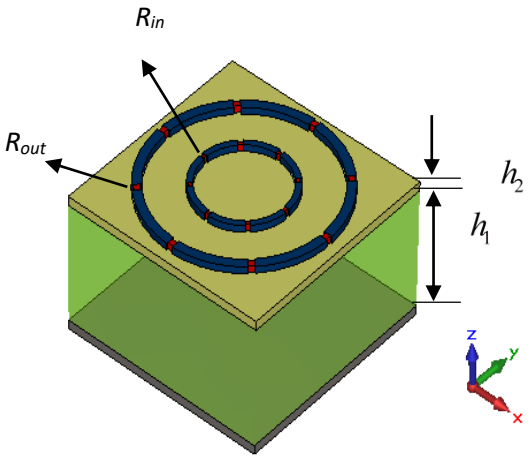

Figure 1: Geometry of the double-circular-loop absorber.

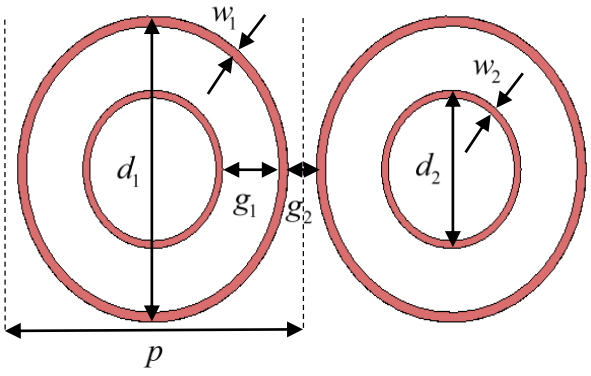

Figure 2: Tow cells of the double circular loops FSS.

TABLE 1
PARAMETERS OF THE DOUBLE CIRCULAR LOOPS FSS

Parameter	Description	Value (mm)
p	Size of the unit cell	3.25
g1	Minimum gap between the circle in two adjacent unit cell	1
d1	Diameter of the outer loop	24
w1	Width of the outer loop	0.4
g2	Gap between inner and outer loops	4.6
d2	Diameter of the inner loop	14
w2	Width of the inner loop	0.5

Accurate modelling for the FSS is a challenging problem over a broad bandwidth for different incident angles and polarizations. Fig. 2 illustrates the geometry of the double circular loops FSS. In each unit cell, there are two printed circular conducting loops. The parameters of the double circular loops FSS are listed in Table 1. The array of double circular loops is represented by LC circuit as shown in Fig. 3. We describe the lumped-element equivalent circuit model for the DCL array and compare the results with those obtained by the full-wave methods.

The modelling is based on equations given by Marcuvitz for periodic arrays of thin conducting strips [13].

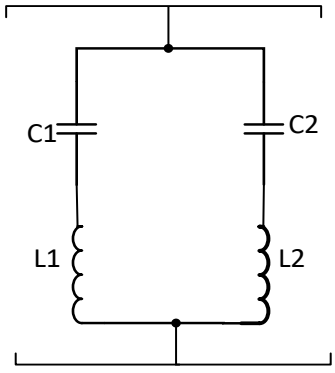

Figure 3: Equivalent circuit model for the double circular loops FSS.

This model can be used where the element geometry is described as inductive and capacitive components. The basic equations to calculate the inductance and capacitance of the strip gratings are [13]:

$$X_{TE} = \frac{p\cos\theta}{\lambda}\left[\ln\cos ec\frac{\pi w}{2p} + G(p,w,\lambda,\theta)\right] \quad (1)$$

$$B_{TM} = \frac{4p\cos\varphi}{\lambda}\left[\ln\cos ec\frac{\pi g}{2p} + G(p,g,\lambda,\varphi)\right] \quad (2)$$

$$X_{TM} = \frac{p\sec\varphi}{\lambda}\left[\ln\cos ec\frac{\pi w}{2p} + G(p,w,\lambda,\varphi)\right] \quad (3)$$

$$B_{TE} = \frac{4p\sec\theta}{\lambda}\left[\ln\cos ec\frac{\pi g}{2p} + G(p,g,\lambda,\theta)\right] \quad (4)$$

where w is the width of each strip, g is the distance between two successive strips. Also, p is the periodicity of the strips, (θ, φ) are the angle of incidence, λ is the wavelength and G is the correction term [13].

Fig. 3 shows the equivalent circuit model derived for the array of double circular loops FSS which consists of two series circuits in parallel. The admittance of the DCL-FSS is calculated using the equivalent circuit as follows.

$$Y = j\omega\left[\frac{C_1 + C_2 - \omega^2 C_1 C_2\left(L_1 + L_2\right)}{\left(1-\omega^2 C_1 L_1\right)\left(1-\omega^2 C_2 L_2\right)}\right] \quad (5)$$

Equivalently, Y can be written in a more compact form as:

$$Y = j\left[\left(\frac{B_1}{1-X_1 B_1}\right) + \left(\frac{B_2}{1-X_2 B_2}\right)\right] \quad (6)$$

The basic equations for calculating the equivalent inductance and capacitance of the double-square-loop FSS is given by Langley et al. [12], [13]. Therefore, we can obtain a lumped-element equivalent circuit model for the double-circular-loop FSS array. The four circuit elements shown in Fig. 3 are given by [18]:

$$X_1 = \omega L_1 = 2.\frac{\pi}{2}.\frac{X_{1p}X_{2p}}{X_{1p}+X_{2p}}.\left(\frac{d_1}{p}\right) \quad (7)$$

$$X_2 = \omega L_2 = \frac{\pi}{2}.F\left(P, 2\omega_2, \lambda\right)\left(\frac{d_2}{p}\right) \quad (8)$$

$$X_{1p} = F(p, w_1, \lambda); X_{2p} = F(p, w_2, \lambda) \quad (9)$$

where a factor π/2 is used owing to the length of the half circular loop compared with the side of the square loop. In addition, capacitances C1 and C2 are given as [18]:

$$B_1 = \omega C_1 = 0.75.\frac{\pi}{4}.B_{1p}.\left(\frac{d_1}{p}\right) \quad (10)$$

$$B_2 = \omega C_2 = \frac{\pi}{4}.\frac{B_{1p}B_{2p}}{B_{1p}+B_{2p}}\left(\frac{d_2}{p}\right) \quad (11)$$

$$B_{1p} = 4.0.\varepsilon_{eff}.F(p, g_a, \lambda); B_{2p} = 4.0.\varepsilon_{eff}.F(p, g_2, \lambda) \quad (12)$$

where a factor π/4 is used owing to the length of the circular loop compared with the square loop. Also, g_a the average gap between two adjacent unit cells, has been explained in [18].

The transmission coefficient τ can now be calculated from the normalized admittance of the array at the normal incidence as follows.

$$|\tau|^2 = \frac{4}{4+|Y|^2} \tag{13}$$

To verify the validity of the equivalent circuit model for the proposed DCL-FSS, we compare the calculated transmission performance of the DCL-FSS based on the parameter values in Table 1. The results of the circuit model are compared to the full-wave simulator, CST Microwave Studio, as shown in Fig. 4. The simulation results of the equivalent circuit model, as shown in Fig. 4, are obtained using the following values: L1=16.78nH, L2=11.08nH, C1= 0.167pF, C2= 0.465pF. The results are in good agreement over the whole frequency range except the location of the second resonance.

B. Equivalent circuit model of the absorber

According to the formulations given in the previous subsection, the equivalent circuit of the DCL-FSS absorber can be represented by two series RLC circuits connected across a transmission line circuit shown in Fig. 5. It is worth mentioning that L1, C1 and R1 represent the equivalent circuit of the outer loop, while L2, C2 and R2 denote the inner loop. These equivalent inductances and capacitances of the DCL-FSS absorber can be evaluated using equations 7 to 12.

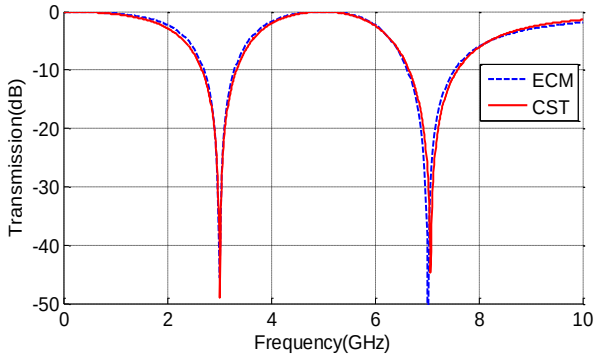

Figure 4: Transmission response of the DCL-FSS calculated from the equivalent circuit model and CST simulation.

The short-circuited transmission line section represents the conductor-backed spacer, i.e. the foam layer, while the short transmission line section denotes the thin substrate, i.e. FR4 layer.

The basic principle operation of the absorber is based on matching the impedance of the absorber layer to the free space impedance. For the transmission line circuit shown in Fig. 5, the reflection coefficient can be written in terms of the input admittance (Y_{in}) and the free space admittance (Y_0) as follows.

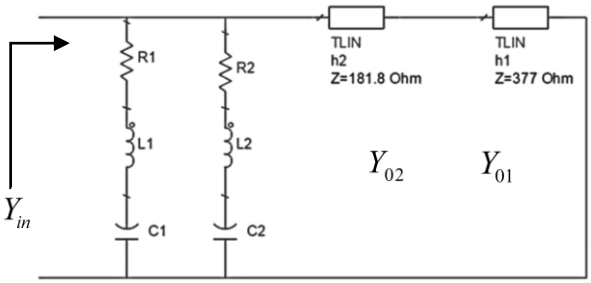

Figure 5: Equivalent circuit model (ECM) of the double-circular-loop FSS absorber.

$$\Gamma = \frac{Y_0 - Y_{in}}{Y_0 + Y_{in}} \tag{14}$$

3. Design Guidelines

Based on the equivalent circuit model, we explain a few design guidelines to obtain a wide-band absorber with high angular stability.

1) A very thin substrate is used for the printed the loops. Here, we choose FR4 with ε_{r2}=4.3 and h_2=0.25mm.

2) Using the center frequency of the absorber, the thickness of the spacer is evaluated similar to Salisbury screen, that is:

$$\beta_1 h_1 + \beta_2 h_2 = \frac{\pi}{2} \tag{15}$$

Using (16), h_1=14.5 mm is obtained for the center frequency of 5GHz.

An efficient optimization can be carried out to determine the physical dimensions of DCL-FSS, i.e. g_1, d_1, w_1, g_2, d_2, w_2, and the resistance of the two loops. Hence, a broad bandwidth for high absorption up to 40° regard to the normal incidence for both polarizations is achieved. After optimization based on the ECM, the design parameters, i.e. g_1, d_1, w_1, g_2, d_2, w_2, of the absorber are listed in Table 2. The values of the lumped capacitances and inductances of the circuit model are then determined using the DCL dimensions. Also, the values of the lumped resistors are determined for desired frequency response. The equivalent inductances, capacitances and resistors of the DCL are obtained and listed in Table 3. The values of the lumped inductances and capacitances are determined from the DCL dimensions according to equations (7-12) and the values of the lumped resistors are determined for the desired frequency response.

To verify the validity of the equivalent circuit model of the DCL-FSS absorber, the simulated reflectivity performance of the resistor-loaded DCL absorber obtained by the circuit model is compared the full-wave

results from CST Microwave Studio, as shown in Fig. 6. It should be mentioned that the dimensions of the DSL absorber are properly chosen to exhibit wideband with high angular stability absorbing performance. Good agreement between the full-wave results and the theoretical prediction of the proposed circuit is observed. Fig. 6 depicts that the EM simulated return loss is more than 10 dB from 1.89 GHz to 8.29 GHz corresponding to the fractional bandwidth of 125.7 % for the normal incidence using the parameters of Table 1 with Res_{in}=75Ω, Res_{out}=120Ω and h_1=14.5mm, h_2=0.25mm. Furthermore, the total thickness of the proposed absorber is 0.093λL, where λ_L is the wavelength at the lowest frequency.

4. Physical Interpretation of the Absorber Design

To design of a DCL-FSS, the proposed equivalent circuit model is used. The physical mechanism of the absorber can help the designer to reach the optimum design with less iterative computer analyses. There are a few number of parameters influencing on the design procedure. The absorption frequency as well as the FSS inductances and capacitances are primarily related to the size of unit cell (p), the diameter of the inner and outer loops (d_1, d_2), the permittivity and thickness of the dielectric substrate, the width of the inner and outer loops (w_1, w_2) and the gap between loops (g_1, g_2). The following subsections discuss the physical mechanisms of the DCL absorber in terms of several important parameters.

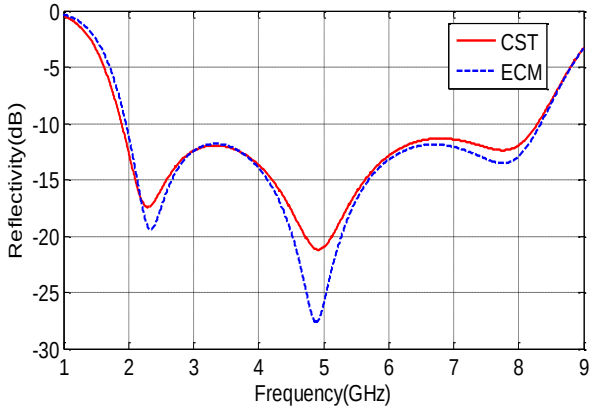

Figure 6: Reflectivity of the DCL FSS absorber calculated by the equivalent circuit model and CST simulator.

Table 2
Physical Dimensions of the DCL FSS

w_1 (mm)	w_2 (mm)	d_1 (mm)	d_2 (mm)	g_1 (mm)	g_2 (mm)
0.4	0.5	24	14	1	4.6

Table 3
Equivalent Elements of the Optimized DCL FSS Absorber

L1 (nH)	L2 (nH)	C1 (pF)	C2 (pF)	R1 (ohm)	R2 (ohm)
16.78	11.08	0.167	0.0465	270	280

It is observed from Fig. 6, that there are three resonances within the operating frequency band for the proposed absorber design.

It should be pointed out that the first resonance occurs before the resonance frequency of the outer loop, the second resonance is very similar to the classic Salisbury screen, where the susceptance produced by the grounded spacer is zero and the third resonance occurs after the resonant frequency of the inner loop.

A. Change of the outer loop width w_1

In this section, all parameters are unchanged expect outer loop width, w_1.

The calculated reflectivity of the absorber for different values of w_1 is given in Fig. 7. Since the resonant frequencies are mainly dependent upon the diameter of the loops, and the loop diameters are unchanged, so the resonant frequencies do not varies with the variation of w_1.

However, the reflectivity reduction level decreases at the first resonant frequency and increases at the center frequency of the absorber when w_1 is reduced. It is then concluded that great reduction of the reflectivity is observed at the resonant frequencies.

B. Change of the inner loop width w_2

In this section, all parameters are unchanged expect inner loop width w_2.

The calculated reflectivity of the absorber as a function of frequency for different values of w_2 is shown in Fig. 8.

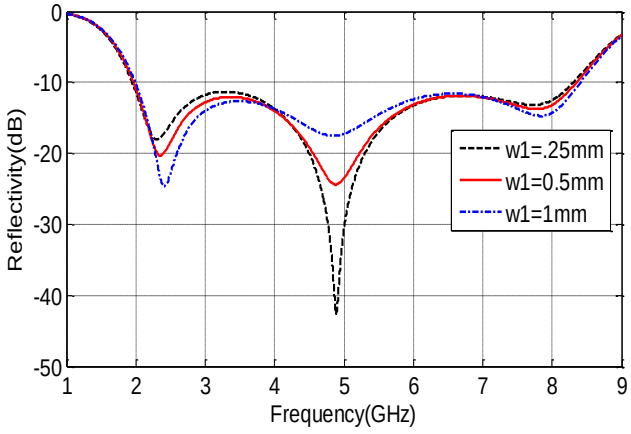

Figure 7: Calculated reflectivity of the DCL-FSS absorber vs. frequency for different values of w_1.

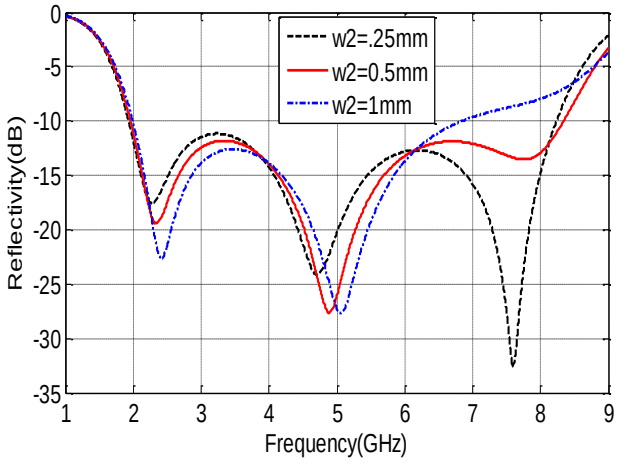

Figure 8: Calculated reflectivity of the DCL-FSS absorber vs. frequency for different values of w_2.

It is seen that the increase of w_2 increases the RCS significantly at the third resonant frequency and it also reduces the RCS at the first resonant frequency. What is more interesting is that the overall bandwidth is reduced when w_2 increases.

C. The inter-element spacing g_1

The inter element spacing g_1 is equal to p-d_1. If the period of the array is kept constant and let the inter-element spacing change, the outer diameter of the outer loop changes, accordingly. From (6) and (7), we observe that inductance L1 and capacitance C1 are inversely proportional to the inter-element spacing g_1, therefore as g_1 is reduced, C1 and L1 are increased. As a result, the first resonant frequency becomes lower. In order to achieve a smaller absorber thickness, small inter element spacing g_1 is preferred. Fig. 9 shows the reflectivity performance of a resistor-loaded DCL-FSS absorber varying with the inter element spacing. As expected, a reduction of g_1 cause the lowest operating frequency of the absorber to decrease and therefore reduces the absorber thickness vs. λ_L.

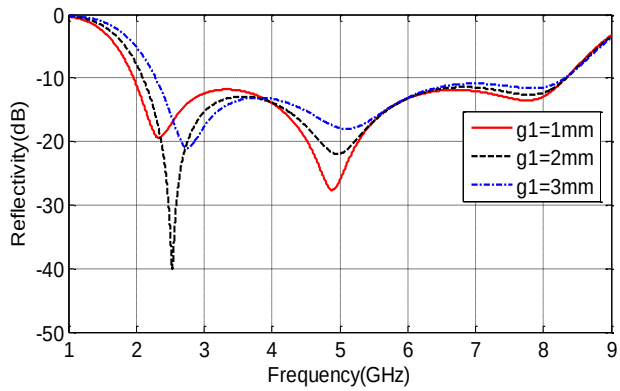

Figure 9: Calculated reflectivity of the DCL-FSS absorber vs. frequency for different values of g_1.

D. Change of the inner loop diameter d_2

Another important parameter of the DCL-FSS absorber model is the radius of the inner circular loop (d_2).

From (6) and (7), we observe that inductance L2 and capacitance C2 are proportional to d_2; consequently, as d2 is reduced, C2 and L2 are increased. As a result, the first resonant frequency remains almost constant but the third resonant frequency becomes lower. Fig. 10 shows the reflectivity performance of a DCL-FSS absorber varying with d_2. It is seen that the first resonance hardly changes but the third resonance decreases with the increase of d_2. Furthermore, the reflectivity near the third resonance is decreased by the increase of d_2. In order to achieve a wideband absorber with small thickness, inner loop diameter of d_2 should be selected carefully to reach the optimum radius ensuring the design goals.

5. Performance of the Proposed DCL FSS Absorber

It is important to study the absorption performance of the proposed absorber under oblique angle of incidences. Simulated reflectivity of the DCL-FSS absorber for both TM and TE polarizations under oblique angle of incidence are shown in Fig. 11. It is observed that the absorption is acceptable up to 40 degrees for 10 dB return loss, therefore the absorber has a wide angle stability.

In order to understand the performance of the proposed absorber compared to existing single-layer absorbers, the angular stability, bandwidth and thickness are expressed in Table 4. A single-layer absorber with a bandwidth of about 98.5% and thickness of $0.112\lambda_L$ was realized in [4]. In [5], an absorber with bandwidth of 112% and thickness of $0.104\lambda_L$ was realized by using a resistive square loop. By using genetic algorithm optimization an absorber with bandwidth of 77.5% and thickness of $0.091\lambda_L$ was designed [6]. A two-dimensional periodic array with unit cells consisting of DSL loaded with series resistances was also proposed in [7] with a bandwidth of 126.8% and a thickness of $0.088\lambda_L$ but the angular stability of this absorber is lower than 30 degrees. In this paper, a new CA absorber with a bandwidth of about 125.7%, thickness of $0.093\lambda_L$ and angular stability of 40 degrees is designed.

6. Conclusion

In this paper, a simple equivalent circuit model based on transmission line and Marcuvitz theory was presented to accurately analyze a CA absorber structure comprising DCL-FSS. Using the circular loop elements, the response of the FSS is very insensitive to large incident angle variations. Also, it has been shown that the array of double-circular-loop FSS has a special

property that enables us to model it very accurately for a large scan angle. All these fascinating properties make the circular loops FSS have significant

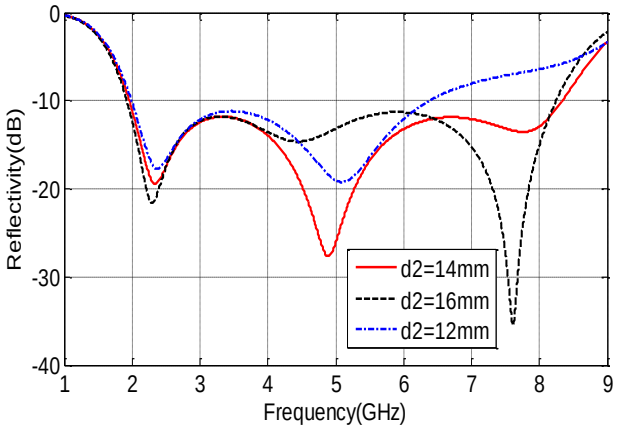

Figure 10: Calculated reflectivity of the double-circular loop absorber vs. frequency for different values of d_2.

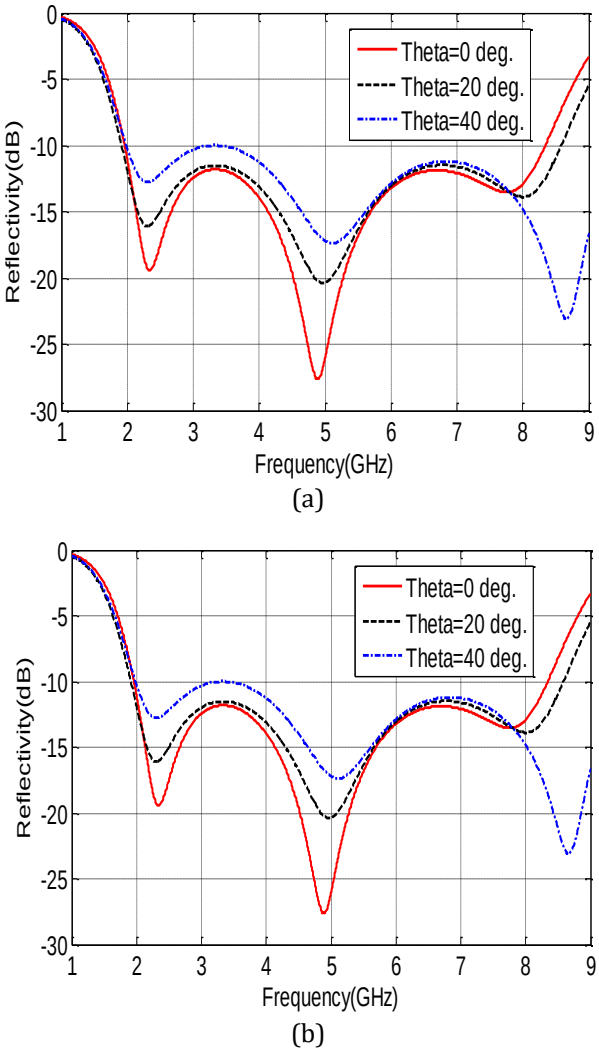

Figure 11: Simulated reflectivity under different oblique incidence angles for (a) TM and (b) TE modes.

TABLE 4
BANDWIDTH, THICKNESS AND ANGULAR STABILITY COMPARISON OF EXISTING CIRCUIT ANALOG ABSORBER

Ref	Fractional bandwidth (%)	Thickness (unit: λ_L)	Angular stability (degrees)
[4]	98.5	6.0.112	7.40
[5]	112	0.104	30
[6]	77.5	0.091	30
[7]	126.8	0.088	30
Our work	125.7	0.093	40

As seen, the angular stability of the DCL-FSS absorber has been improved due to using the circular loops.

performance in comparison to the earlier published designs.

The dimensions of the unit-cell FSS are related to the parallel circuits, and their effects on the absorption frequency have been investigated. The variations of substrate thickness and FSS parameters have been studied for optimizing the absorber bandwidth and thickness for a high range of incident angles and different polarizations. The calculated result matches well with the simulated responses with minor deviation. The proposed equivalent circuit can be considered as a generalized model for analyzing absorber structures of DCL-shaped frequency selective surfaces. The proposed absorber has a reduction of reflectivity more than 10dB with the relative bandwidth of 125.7%. Moreover, the reflectivity of the proposed absorber has excellent stability with respect to TE and TM polarizations and different incident angles up to 40 degrees.

REFERENCES

[1] E. F. Knott, J. F. Shaeffer, and M. T. Tuley, *Radar Cross Section*, 2nd ed. Raleigh, NC, USA: SciTech, 2004.

[2] B. A. Munk, *Frequency Selective Surfaces Theory and Design*, New York, John Wiley & Sons Inc., 2000.

[3] K.N. Rozanov, "Ultimate thickness to bandwidth ratio of radar absorbers," *IEEE Trans. Antennas Prop.*, vol. 48, no. 8, pp. 1230–1234, Aug. 2000.

[4] A. Kazemzadeh, "Nonmagnetic ultra wideband absorber with optimal thickness," *IEEE Trans. Antennas Prop.*, vol. 59, no. 1, pp. 135–140, 2011.

[5] F. Costa, A. Monorchio, and G. Manara, "Analysis and design of ultra-thin electromagnetic absorbers comprising resistively loaded high impedance surface," *IEEE Trans. Antennas Prop.*, vol. 58, no. 5, pp. 1551-58, May 2010.

[6] H. Choo, H. Ling, and C. S. Liang, "On a class of planar absorbers with periodic square resistive patches," *IEEE Trans. Antennas Prop.*, vol. 56, no. 5, pp. 2127-2130, 2008.

[7] Y. Shang, Z. Shen, and S. Xiao, "On the design of single-layer circuit analog absorber using double-square-loop array," *IEEE Trans. Antennas Prop.*, vol. 61, no. 12, pp. 6022-6029, 2013.

[8] M. Li, S. Xiao, Y. Bai, and B. Wang, "An ultrathin and broadband radar absorber using resistive FSS," *IEEE Antennas Wireless Prop. Lett.*, vol. 11, pp. 748–751, Dec. 2012.

[9] N. Liu, X. Sheng, C. Zhang, J. Fan, and D. Guo, "A design method for synthesizing wideband band-stop FSS via its equivalent circuit model," *IEEE Antennas and Wireless Propagation Letters*, vol. 16, pp. 2721-2725, 2017.

[10] C. C. Chen, "Transmission through a conductive screen perforated periodically with apertures," *IEEE Transactions on Microwave Theory and Technology,* vol. MTT-18, no. 9, pp. 627-632, September 1970.

[11] R. Mittra, C. H. Chan, and T. C. wick, "Techniques for analyzing frequency selective surfaces a review," *IEEE Proceedings*, vol. 76, pp. 1593-1615, 1988.

[12] R. J. Langley and E. A. Parker, "Equivalent circuit model for arrays of square loops," *Electron. Lett.*, vol. 18, no. 7, pp. 294–296, Apr. 1982.

[13] R. J. Langley and A. J. Drinkwater, "Improved empirical model for the Jerusalem cross," *Microwaves*, *Antennas and Propagation*, *IEE Proceedings H*, vol. 129, no. 1, pp 1-6, 1982.

[14] S. Narayan, B. Sangeetha, T. V. Sruthi, V. Shambulingappa, and R. Unnikrishnan Nair, "Design of low observable antenna using active hybrid-element FSS structure for stealth applications," *International Journal of Electronics and Communications (AEÜ)*, vol. 80, pp. 137-143, 2017.

[15] R. J. Langley and E. A. Parker, "Double-square frequency-selective surfaces and their equivalent circuit," *Electron. Lett.*, vol. 19, no. 17, pp. 675–676, Aug. 1983.

[16] N. Marcuvitz., *Waveguide Handbook*, McGraw-Hill, New York, 1951.

[17] I. K. Anderson, On the theory of self-resonant grids, *The Bell System Technical Journal*, vol. 54, pp. 1725-1731, 1975.

[18] A. Ramezani Varkani, Z. H. Firouzeh, and A. Zeidaabdi-Nezhad, "Equivalent circuit model for array of circular loop FSS structures at oblique angles of incidence," *IET Microwaves, Antennas & Propagation,* vol. 12, no. 5, pp. 749-755, 2018.

BIOGRAPHIES



Mojtaba Basravi received the B.Sc. degree in Electronics Engineering from the Malek-Ashtar University of Technology, Isfahan, Iran, in 2012, and received the M.Sc. degree in Communications Engineering from Isfahan University of Technology, Isfahan, Iran, in 2016. His research interests include designing of low-RCS antennas and arrays, frequency selective surfaces and radar absorbing materials.



Zaker Hossein Firouzeh received the B.Sc. degree in Electrical Engineering from Isfahan University of Technology (IUT), Isfahan, in 1999 and the M.Sc. and Ph.D. degrees in Electrical Engineering from Amirkabir University of Technology (AUT), Tehran, Iran, in 2002, and 2011, respectively. He was a Research Engineer at Information Communication Technology Institute (ICTI) of IUT from 2002 to 2006. He experienced in design and implementation of antenna, Radar, and wireless communication systems. His current research interests include antenna design and measurements, numerical techniques in electromagnetics, wave propagation and scattering, and EMC/EMI.



Mohsen Maddahali received the B.Sc. degree in Electronics and Telecommunications from Isfahan University of Technology (IUT), Isfahan, Iran, in 2005 and the M.Sc. and Ph.D. degrees in Electrical Engineering from Tarbiat Modares University, Tehran, Iran, in 2008 and 2012, respectively. Since 2012, he has been an Assistant Professor with the Department of Electrical and Computer Engineering, IUT. His research interests include computational electromagnetics, antenna theory, array antennas and phase array antennas.

How to cite this paper:

M. Basravi, Z. H. Firouzeh, and M. Maddahali, "Design of a single-layer circuit analog absorber using double-circular-loop array via the equivalent circuit model," Journal of Electrical and Computer Engineering Innovations, vol. 5, no. 2, pp. 171-178, 2017.

DOI: 10.22061/JECEI.2018.790

URL: http://jecei.sru.ac.ir/article_790.html